SLAC–PUB–7735
January 1998

Electron-Cloud Effects in High-Luminosity Colliders*

F. Zimmermann
Stanford Linear Accelerator Center
Stanford University, Stanford, CA 94309, USA

Electron-cloud instabilities are expected to be important in most high-luminosity double-ring colliders. In this report, I describe a few parameter regimes and some critical parameter dependences of this type of instability, and illustrate these with simulation results for the PEP-II and KEK B factories, the LHC, the VLHC, and DAPHNE. In addition, I study the possibility and the potential impact of an electron cloud in the interaction region.

Presented at the Advanced ICFA Beam Dynamics Workshop on Beam Dynamics Issues for e^+e^- Factories Frascati, Italy, October 20–25, 1997

*Work supported by the U.S. Department of Energy contract DE–AC03–76SF00515.

ELECTRON-CLOUD EFFECTS IN HIGH-LUMINOSITY COLLIDERS*

F. Zimmermann
Stanford Linear Accelerator Center, Stanford, California 94309

ABSTRACT

Electron-cloud instabilities are expected to be important in most high-luminosity double-ring colliders. In this report, I describe a few parameter regimes and some critical parameter dependences of this type of instability, and illustrate these with simulation results for the PEP-II and KEK B factories, the LHC, the VLHC, and DAPHNE. In addition, I study the possibility and the potential impact of an electron cloud in the interaction region.

1 Introduction

The new generation of high-luminosity e^+e^- factories is characterized by many bunches with small bunch spacings and by the use of double rings. In the positron rings of these machines, photoelectrons produced by synchrotron radiation are attracted by the field of the beam, with which they can strongly interact. An electron-cloud instability was first observed and identified at the KEK photon factory [1, 2]. Meanwhile, evidence for such instabilities is also reported from BEPC in Bejing [3] and from CESR [4]. Recent studies suggest [5, 6, 7] that this instability could limit the performance of the two B factories under construction at SLAC and KEK.

This work was supported by the U.S. Department of Energy under Contract No. DE-AC03-76SF00515.

Electron-cloud instabilities are predicted to occur not only in positron rings, but also in the highest-energy proton colliders: the LHC [8, 9, 10] and the VLHC [11]. Very similar to the e^+e^- factories, these proton machines are designed as double rings and their bunch spacings are comparable. In addition, they will be the first proton colliders with significant synchrotron radiation: The relativistic factor $\gamma = E/(mc^2)$ for the LHC is the same as for the low energy ring of the SLAC PEP-II B factory. Thus, the number of photons emitted per turn is identical. In the LHC the electron-cloud effect is compounded by the absence of an antechamber and by a critical photon energy of about 50 eV which is close to the energy of maximum photoemission yield.

The build-up of an electron cloud starts with photoemission from the vacuum-chamber wall. The photoelectrons are accelerated by the beam field to an energy of a few hundred eV, which is sufficiently high that they induce secondary emission when they again hit the wall. After the passage of a few bunches, the electron cloud acquires a quasi-stationary density distribution, determined by the photoemission, the secondary emission, its own space-charge field and by the accelerating bunch charge. The response of the cloud to a perturbation in the transverse beam position can couple the motion of successive bunches and is similar to a wakefield. Once an electron cloud has built up in the beam pipe, it can give rise not only to multi-bunch instabilities, but also to emittance dilution (even if the dipole instability is damped by a feedback), to an increased heat load on the cryogenic system (in the case of superconducting magnets, for example in the LHC), and, finally, to an increased background in the experiments.

The results of computer simulations modeling the electron-cloud effects are very sensitive to many properties of the vacuum chamber which are not well known. This introduces a large uncertainty into all our predictions.

2 Parameter Regimes, Dependences and Rise-Time Estimates

An important parameter characterizing the nature of the electron-cloud effect is the ratio of the minimum photoelectron travel time across the beam pipe to the bunch spacing [12], $n_{min} \equiv r^2/(N_b r_e L_{sep})$, where r denotes the half height of the beam pipe, N_b the number of particles per bunch, r_e the classical electron radius, and L_{sep} the bunch separation. Table 1 shows that the values of n_{min} vary from 0.2 for the LHC to 40 for KEKB. This means that in the LHC almost all primary photoelectrons have been lost when the next bunch arrives, and the wakefield information is almost entirely carried by the secondary electrons, whereas photoelectrons in KEKB or PEP-II experience several bunch passages, before they hit the beam pipe. The first case can be called the multipacting regime [13]; the second is the regime of the

Table 1: *Selected parameters for a few storage rings.*
**For $N_b = 4.5 \times 10^9$, the predicted rise time for a drift space in DAPHNE is 2 ms.*

accelerator	LHC	VLHC	DAPHNE	PEP-II	KEKB
beam energy E [GeV]	7000	50000	0.51	3.1	8
bunch population N_b [10^{10}]	10	1	9	6	3.3
no. of bunches n_b	2835	10^5	120	1658	5000
betatron tune $Q_{x,y}$	63	247	4.5, 6.1	35	46
rms beam sizes $\sigma_{x,y}$ [mm]	0.3	0.09	1.9, 0.16	1.4, 0.2	0.64, 0.08
bunch spacing [m]	7.5	5.2	0.81	1.26	0.59
chamber half height r [mm]	20	9	20	25	47
chamber material/coat.	Cu	Al	Al	TiN	Cu
antechamber	no	no	yes	yes	no
sec. emission yield δ_{max}	>1.5	>2.5	>2.5	1.1	> 1.2
parameter n_{min}	0.2	0.6	2.0	3.1	40
pred. rise time $\tau_{x,y}$ [ms]	50, 400	3000	$< 0.01^*$	0.3, 0.5	0.06

original 'Ohmi effect' [2]. Though the dynamics in the two cases is quite different, there is a smooth transition between the two. For example, since n_{min} is a function of the bunch population, at lower current, *e.g.*, during commissioning, the LHC might well operate in the Ohmi regime.

Aside from the bunch-spacing/transit-time ratio, electron-cloud effects can be further classified according to: 1) the type of magnetic (or electric) field in which they occur (*e.g.*, bending magnets, drifts, solenoids, ion-pump fields...), 2) the vacuum-chamber material and geometry (*e.g.*, reflectivity, secondary-emission and photoemission yields, energy distribution of the secondaries and photoelectrons...), and 3) the presence or absence of an antechamber.

The electron-cloud induced wakefield is influenced by many parameters. In Fig. 1 we illustrate the dependence on the secondary-emission yield parameter [14] δ_{max}, on the bunch current, and on the energy distribution of the secondary electrons [15] with four simulation results for the VLHC, for PEP-II/KEKB and for the LHC[1].

Assuming a rapidly decaying 'wake', the instability rise time is [16]

$$\tau_{x,y} \approx \frac{4\pi\gamma Q_{x,y}}{N_b r_p c W_{x,y}(L_{sep})} \tag{1}$$

where $Q_{x,y}$ denotes the betatron tune and $W_{x,y}(L_{sep})$ the bunch-to-bunch wake function obtained from the simulation. Some rise-time estimates are listed in Table 1.

[1]The physics model of the simulation code was described in Refs. [8] and [9].

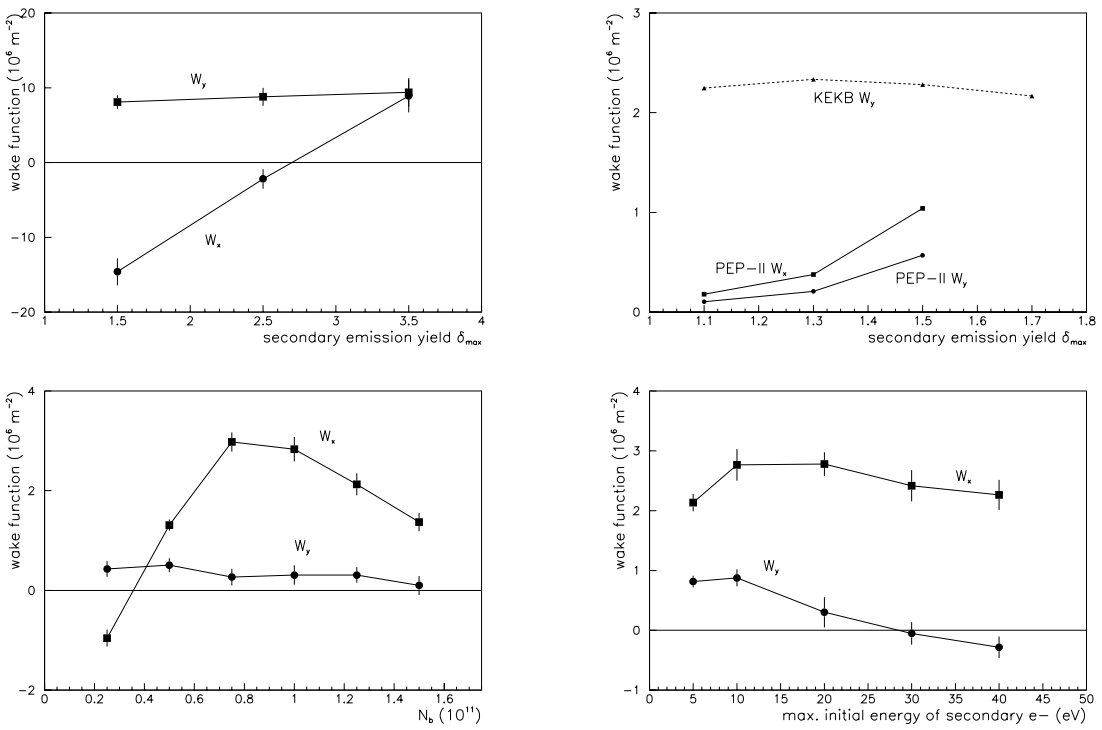

Figure 1: *Simulated effective wake function: (top left) vs. the maximum secondary emission yield for perpendicular incidence δ_{max} in the VLHC; (top right) vs δ_{max} in PEP-II and KEKB; (bottom left) vs. the bunch population for the LHC; (bottom right) vs. the maximum initial energy of the secondary electrons in the LHC.*

3 Electrons in the Interaction Region

Even if the interaction region is perfectly shielded against all sources of synchrotron radiation, there is always a certain number of electrons generated via collisional ionization by the particle beams. The number of electrons generated over a length L around the interaction point is about $N_{e-} \approx 6 n_b N_b L p$ [Torr] per turn. Using PEP-II parameters, $p \approx 8$ nTorr and $L \approx 30$ cm, we find $N_{e-} \approx 1.5 \times 10^6$ e$^-$ per turn or $dN_{e-}/dt \approx 2 \times 10^{11}$ s^{-1}. These electrons, after being accelerated by the beam field, can potentially contribute to the detector background or to the heat load of the vertex detector or of other critical components [17]. In case of PEP-II, the motion of the electrons is constrained transversely by a 1.5-T longitudinal solenoid field[2]. At a distance of about 20 cm from the IP, the solenoid field is superimposed with a 0.7-T permanent horizontal bending magnet. This field combination guides the electrons downwards onto the permanent magnet, which they will hit within an area

[2]Trapped electrons spiraling in this solenoid field, like in an ion pump, could significantly increase the ion production rate, an additional complication which has not yet been studied.

of approximate size $A \approx 2\pi(\sigma_x^{*\,2} + L^2\theta_x^{*\,2})^{1/2} L\theta_y^* \approx 0.1$ mm^2, where $\sigma_x^* \approx 155$ μm and $\theta_x^* \approx \theta_y^* \approx 420$ μrad denote the rms horizontal IP spot size and the rms IP divergences, respectively.

Figure 2 depicts the energy distribution of the electrons incident on the permanent bending magnet, as obtained from 2 preliminary simulation studies. Average electron energies are of the order of 0.5–2 keV, translating into a total energy deposition of 0.6–3.2 GeV per turn or 130–700 μW/mm^2. This is comparable to the energy deposition in the entire interaction region by beam particles lost due to gas scattering [18]. However, since the average energy of the lost ionization electrons is very moderate, their contribution to the background may be much less important.

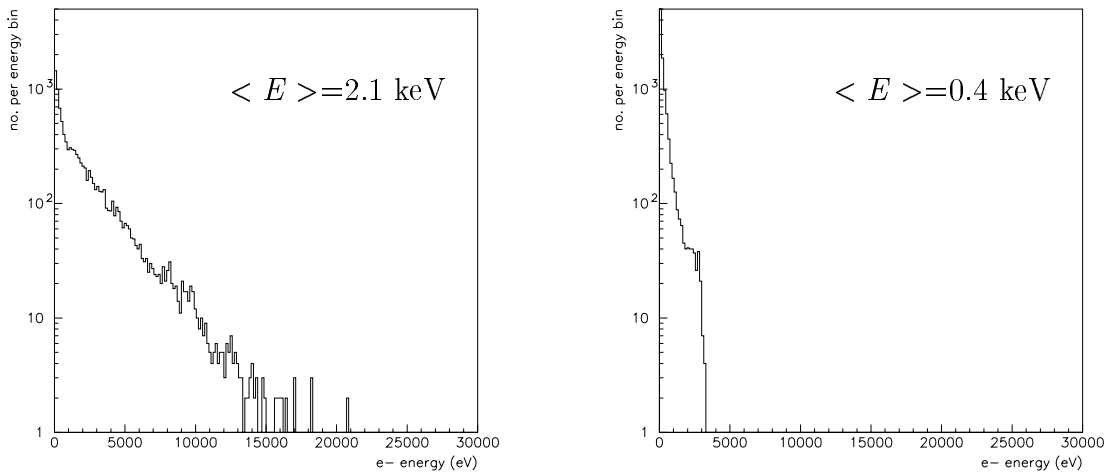

Figure 2: *Energy distribution of interaction-region electrons hitting the upper side of the permanent bending magnet B1, about 30 cm from the PEP-II IP: (left) for* $N_b^{e^+} \approx 6 \times 10^{10}$ *and simulating a drift space; (right) for* $N_b^{e^+} \approx 6 \times 10^{10}/4$ *(one factor of 2 comes from the geometry, another factor of 2 from an assumed partial field cancellation by the electron beam) and a 0.7-T vertical dipole field.*

4 Conclusions

In modern colliders, electron-cloud effects are ubiquitous. They lead to instabilities, to emittance growth, and, in case of the LHC, to an increased heat load on the cryogenic system. Electrons generated and lost in the interaction region may also cause background and/or a local overheating of components. The simulated wakefield depends on many parameters. A good knowledge of material and surface properties of the vacuum chamber is essential for reliable predictions.

Acknowledgements

I would like to thank F. Ruggiero, S. Mitsunobu, M. Furman, S. Heifets, T. Raubenheimer, O. Gröbner, C. Benvenuti, J. Gareyte, G. Lambertson, J. Seeman, R. Kirby, M. Zisman, W. Stoeffl and E. Malamud for helpful discussions and suggestions.

References

1. M. Izawa et al., Phys. Rev. Lett., Vol. 74, No. 8 (1995).
2. K. Ohmi, Phys. Rev. Lett., Vol. 75, No. 8 (1995).
3. Z.Y. Guo, talk at MBI97 workshop, July 1997, KEK, Tsukuba, Japan.
4. J. Rogers, talk at MBI97 workshop, July 1997, KEK, Tsukuba, Japan.
5. M. Furman and G. Lambertson, IEEE PAC97 Vancouver, LBL-40256 (1997).
6. S.A. Heifets, SLAC/AP-95-101 (1995).
7. K. Ohmi, talk at MBI97 workshop, July 1997, KEK, Tsukuba, Japan.
8. F. Zimmermann, CERN LHC Project Report 95 and SLAC-PUB-7425 (1997).
9. F. Zimmermann, talk at MBI97 workshop, July 1997, KEK, Tsukuba, Japan, and SLAC-PUB-7664 (1997).
10. A.V. Burov and N.S. Dikansky, talk at MBI97 workshop, July 1997, KEK, Tsukuba, Japan.
11. F. Zimmermann, SLAC/AAS-91 (1997).
12. O. Gröbner, "Beam-Induced Multipacting", IEEE PAC97 Vancouver (1997).
13. O. Gröbner, Vacuum, vol. 47, pp. 591–595 (1996).
14. H. Seiler, J. Appl. Phys. 54 (11) (1983).
15. S. Mitsunobu, private suggestion (1997).
16. A. Chao, "Physics of Collective Beam Instabilities in High Energy Accelerators", Wiley, p. 208 (1995).
17. S. Mitsunobu, private communication (1997).
18. BABAR Technical Design Report, SLAC-R-95-457, Fig. 12-6 (1995).